

SAND97-8497 • UC-404
Unlimited Release
Printed June 1997

Determination of Modified Embedded
Atom Method Parameters for Nickel

(To be published in the journal Materials Chemistry and Physics)

M. I. Baskes

Prepared by
Sandia National Laboratories
Albuquerque, New Mexico 87185 and Livermore, California 94551
for the United States Department of Energy
under Contract DE-AC04-94AL85000

Approved for public release; distribution is unlimited.

**DETERMINATION OF MODIFIED EMBEDDED ATOM METHOD PARAMETERS FOR
NICKEL**

M. I. Baskes
Materials Reliability Department
Sandia National Laboratories/California

ABSTRACT

The Modified Embedded Atom Method (MEAM) is an empirical extension of the Embedded Atom Method (EAM) that includes angular forces. A detailed study is presented to show the effect of various MEAM parameters on the calculated properties of a model material, nickel. Over 50 physical properties of nickel are calculated for four MEAM potentials. It is found that, in general, the predicted material properties are extremely insensitive to the parameter variations examined. In a few cases: interstitial migration; the (110) surface reconstruction; and the coefficient of thermal expansion, significant effects of potential were found. Minor differences were also found for the vacancy migration energy, the interstitial formation energy, and the stability of the bcc structure. These results point out the appropriate experimental measurements or first principles calculations that need to be performed to obtain a reliable MEAM parameter set. This work results in a MEAM potential that reproduces all of the experimental data examined.

DETERMINATION OF MODIFIED EMBEDDED ATOM METHOD PARAMETERS FOR NICKEL*

1. Introduction

It is well known that the Embedded Atom Method (EAM) is able to reproduce physical properties of many metals[1]. Unfortunately the use of the EAM is restricted to materials in which angular bonding is unimportant[2]. The modified EAM (MEAM) proposed by Baskes et al.[3-5] was developed to extend the application to materials with all types of bonding. The development of MEAM, however, is not as rigorous as the EAM. Even though most of the MEAM parameters are closely connected to direct experimental observables, a number of them are not. In the past these parameters have been chosen in an ad-hoc way[5]. In addition, a number of forms for the angularly dependent electron density have been used[5-9] as well as a number of screening functions [5, 10]. The purpose of this manuscript is to examine the effects of the above assumptions carefully. Specifically, we intend to examine the sensitivity of numerous calculated physical quantities to 1) ad-hoc parameters, 2) the form of the background electron density, and 3) the range of the many body screening function. We will restrict our study to a single material, nickel. We recognize that nickel is usually thought of a material in which the angular bonding is unimportant. EAM potentials describe nickel quite well. However, angular forces do exist in nickel to the extent of allowing us to test the MEAM parameter dependence. Our choice of nickel is based on the fact that there is a large body of experimental data with which to compare our results. Clearly future work should examine the MEAM parameters in a strongly angularly dependent material such as silicon.

In the body of the manuscript below, we will first review the MEAM formalism. Then the four nickel MEAM potentials will be discussed and applied to the calculation of a number of physical properties. A short summary is then provided.

* Dedicated to Professor Masao Doyama on his 70th birthday.

2. Theory

2.1. The model

The total energy, E , of a system of a single type of atoms in the EAM has been shown [11] to be given by an approximation of the form:

$$E = \sum_i \left(F(\bar{r}_i) + \frac{1}{2} \sum_{j \neq i} f(R_{ij}) \right) \quad (1)$$

where the sums are over the atoms i and j . In this approximation, the embedding function F is the energy required to embed an atom into the background electron density at site i , \bar{r}_i ; and f is the pair interaction between atoms whose separation is given by R_{ij} . In the EAM, \bar{r}_i is given by a linear supposition of spherically averaged atomic electron densities, while in the Modified Embedded Atom Method (MEAM), \bar{r}_i is augmented by angularly dependent terms [3-5].

The pair potential between two atoms $f(R)$ separated by a distance R is given by:

$$f(R) = \frac{2}{Z} \{ E''(R) - F(\bar{r}^0(R)) \}. \quad (2)$$

where $\bar{r}^0(R)$ is the background electron density for the reference structure, and Z is the number of first neighbors. Here $E''(R)$ is the energy per atom of the reference structure as a function of nearest neighbor distance R , obtained, e.g., from first principles calculations or the universal equation of state of Rose et al. [12]. Here we choose the latter:

$$E''(R) = -E_c(1 + a^*)e^{-a^*} \quad (3)$$

with

$$a^* = a \left(\frac{R}{r_e} - 1 \right) \quad (4)$$

and

$$a^2 = \frac{9\Omega B}{E_c} \quad (5)$$

where E_c , r_e , Ω , and B are the cohesive energy, nearest-neighbor distance, atomic volume, and bulk modulus, respectively, all evaluated at equilibrium in the reference structure. In this work the reference structure will be taken as fcc, resulting in:

$$\bar{\Gamma}^0(R) = Z\Gamma^{a(0)}(R) \quad (6)$$

where $\Gamma^{a(0)}$ is an atomic electron density discussed below.

In the MEAM the embedding function $F(\bar{\Gamma})$ is taken as:

$$F(\bar{\Gamma}) = AE_c \frac{\bar{\Gamma}}{\Gamma_0} \ln \frac{\bar{\Gamma}}{\Gamma_0} \quad (7)$$

where A is an adjustable parameter and Γ_0 is a density scaling parameter. For this work (fcc reference structure) $\Gamma_0 = Z = 12$.

The background electron density at a specific site, $\bar{\Gamma}$, is assumed to be a function of what we call partial electron densities. These partial electron densities contain the angular information in the model. The spherically symmetric partial electron density $\Gamma^{(0)}$ is the background electron density in the EAM:

$$\Gamma^{(0)} = \sum_i \Gamma^{a(0)}(r^i) \quad (8a)$$

where the sum is over all atoms i not including the atom at the specific site of interest and r^i is the distance from an atom i to the site of interest. The angular contributions to the density are given by similar formulas weighted by the x, y, and z projections of the distances between atoms:

$$(\Gamma^{(1)})^2 = \sum_a \left[\sum_i \Gamma^{a(1)}(r^i) \frac{r_a^i}{r^i} \right]^2 \quad (8b)$$

$$(\Gamma^{(2)})^2 = \sum_{a,b} \left[\sum_i \Gamma^{a(2)}(r^i) \frac{r_a^i r_b^i}{r^{i^2}} \right]^2 - \frac{1}{3} \sum_i [\Gamma^{a(2)}(r^i)]^2 \quad (8c)$$

$$(\Gamma^{(3)})^2 = \sum_{a,b,g} \left[\sum_i \Gamma^{a(3)}(r^i) \frac{r_a^i r_b^i r_g^i}{r^{i^3}} \right]^2 \quad (8d)$$

Here, the $r^{a(h)}$ are atomic electron densities which represent the decrease in the contribution with distance r^i from the site of interest, and the a, b, and g summations are each over the three coordinate directions with r_a^i being the distance from the site in question in that direction. The functional forms for the partial electron densities were chosen to be translationally and rotationally invariant and equal to zero for crystals with cubic symmetry. It has been shown that the forms chosen in Eq. (8) are related to powers of the cosine of the angle between groups of three atoms[4]. Finally, atomic electron densities are assumed to decrease exponentially, i.e.,

$$r^{a(h)}(R) = e^{-b^{(h)}(R/r_c-1)} \quad (9)$$

where the decay lengths, $b^{(h)}$, are constants. To obtain the background electron density from the partial electron densities we make the assumption that the angular terms are a small correction to the EAM. We combine the angular dependence into one term:

$$\Gamma = \sum_{h=1}^3 t^{(h)} (r^{(h)}/r^{(0)})^2 \quad (10)$$

where $t^{(h)}$ are constants. The background density is then taken as:

$$\bar{r} = r^{(0)}G(\Gamma) \quad (11)$$

In the limit of no angular dependence $\Gamma = 0$ and to recover the EAM we must have $G(0) = 1$. We also choose $G'(0) = 1/2$ in any functions we use so that properties, e.g. elastic constants, calculated at the perfect lattice are independent of the functional form of G . Previously three forms of G have been investigated :

$$G(\Gamma) = \sqrt{1+\Gamma} \quad (12a)$$

$$G(\Gamma) = e^{\Gamma/2} \quad (12b)$$

$$G(\Gamma) = \frac{2}{1+e^{-\Gamma}} \quad (12c)$$

The form used in Eq. (12a) was used in the initial formulation[5]. This form has the unfortunate consequence that it yields imaginary electron densities for $\Gamma < -1$ which is possible if any of the $t^{(h)}$ are less than zero. In order to correct this difficulty, the form in Eq. (12b) was used by Baskes[7] and Huang

et al.[8] and the form in Eq. (12c), by Ravelo and Baskes[9, 13]. No controlled studies of the effect of the form of the background electron density were performed previously, but will be presented here.

2.2 Many body screening

It is traditional in implementing EAM type models to limit the range of interaction. Usually that is done by smoothly truncating the radial functions near a cutoff separation. The justification of this procedure is that forces die off with distance and it makes little difference if the small forces on atoms at a large distance are ignored. However, this view is not universal. Calculations involving long-range pseudopotentials or electrostatic forces cannot use a short range radial cutoff. Baskes[5] proposed a different scheme where an additional limitation of the function interactions was imposed using a many body screening function. Here, the justification is that an atom between two other atoms is able to screen the interaction between the outer atoms, hence reducing the force. The suggested implementation in the original manuscript[5] introduced a discontinuity in the screening function which leads to infinite forces. A later implementation[10] has been found to work quite well and is presented below. Let us define a many body screening function S_{ik} that quantifies the screening between two atoms i and k due to other atoms in the system, j . We multiply the atomic electron densities and the pair potential by this function; hence if the atoms are unscreened, $S_{ik} = 1$ and if they are completely screened, $S_{ik} = 0$. The screening function depends on all of the other atoms in the system:

$$S_{ik} = \prod_{j \neq i, k} S_{ijk} \quad (13)$$

where S_{ijk} is calculated using a simple geometric construction. Consider the ellipse (see Fig. 1) passing through atoms i , j , and k with the minor axis of the ellipse determined by atoms i and k . The equation of the ellipse is given by:

$$x^2 + \frac{1}{C} y^2 = \left(\frac{1}{2} r_{ik}\right)^2 \quad (14)$$

where the parameter C is determined by:

$$C = \frac{2(X_{ij} + X_{jk})(X_{ij} - X_{jk})^2 - 1}{1 - (X_{ij} - X_{jk})^2} \quad (15)$$

where $X_{ij} = (r_{ij}/r_{ik})^2$ and $X_{jk} = (r_{jk}/r_{ik})^2$. The r 's are the distance between the respective atoms. We define the screening factor to be a smooth function of C :

$$S_{ijk} = f_c[(C - C_{\min})/(C_{\max} - C_{\min})] \quad (16)$$

where C_{\min} and C_{\max} are the limiting values of C as seen in the ellipses in Fig. 1 and the smooth cutoff function is:

$$f_c(x) = \begin{cases} 1 & x \geq 1 \\ \frac{1}{2} \left(1 - (1 - x)^4 \right) & 0 < x < 1 \\ 0 & x \leq 0 \end{cases} \quad (17)$$

For convenience we also apply a radial cutoff function to the atomic electron densities and pair potential which is given by $f_c[(r_c - r)/\Delta r]$ where r_c is the cutoff distance and Δr gives the cutoff region.

2.3 Potentials

The determination of the parameters has been discussed previously in great detail[5]. Basically, analytic expressions are obtained for the elastic constants, vacancy formation energy, and structural energy differences. Using these expressions and experimental data most of the parameters (or sets of parameters) are uniquely defined. However a number of the $b^{(h)}$ ($h=1$ and 3) parameters and screening parameters are not well determined and nominal values have previously been chosen for convenience. The parameters that are well determined will form the base that will be kept constant in the study presented here. These parameters are given in Table 1. We choose a radial cutoff r_c of 4 Å for all of the potentials. This cutoff is large enough so that in all of the calculations the many body screening dominates the radial cutoff. The cutoff region is taken to be 0.1 Å in all cases. For the many body screening we choose $C_{\max} = 2.8$. This value ensures that for the fcc structure first neighbors are completely unscreened even for reasonably large thermal vibrations. The remaining parameters are given in Table 2 for the four potentials considered here. For potentials 1 and 2 we take the values of $b^{(h)}$ ($h=1$

and 3) used in Baskes[5] while for potentials 3 and 4 we reduce the values to investigate the effect on free surface relaxation. For potentials 1-3 we choose C_{\min} as in Baskes[5]. This choice ensures that the interactions are first neighbor only even in the bcc structure. For potential 4 we reduce C_{\min} so that second neighbors in the fcc structure are not completely screened. For potential 1 we choose the form of the background electron density to be given by Eq. (12a) while for the remaining potentials we choose the form of Eq. (12c).

3. Results and Discussion

3.1 Technique

Using the energetics described above we calculate a large number of properties of nickel using the four potentials. The calculations use standard energy minimization and molecular dynamics (MD) techniques. Cell sizes were chosen to ensure that boundary effects were unimportant with the minimum cell dimension being at least $2 r_c$. In all cases to make results directly comparable, we used the same cell size for the four potentials. To calculate migration energies the saddle point was calculated by moving an atom along the path between two equilibrium positions and relaxing the other atoms. The maximum energy found was taken to be the saddle point.

3.2 Bulk properties

In Table 3 we present the results of the calculations of some properties of bulk nickel in various crystal structures. The properties that are followed by an asterisk are those that were initially fit for potential 1. Experimental values are included for reference. The experimental elastic constants presented here are slightly different than those fit in Ref. [5]. We note that all of the fit properties except for the bcc cohesive energy remain essentially unchanged as we modify the potential. This result is anticipated as we have not modified any potential near equilibrium. As expected the calculated bcc properties change in potential 4 where the range of the potential is increased to include second nearest neighbors. Even in this case the change is moderate (~ 0.1 eV). The expected decrease in cohesive energy and nearest neighbor distance with coordination (fcc=12, bcc=8, sc=6, dc=4) is reproduced by all four potentials.

The c/a for hcp is predicted to be near the ideal value for all four potentials. We also see that extending the range of interaction changes the predicted coefficient of thermal expansion. Potentials 1-3 strongly underestimate this quantity, while potential 4 predicts a result very close to experiment [14]. Note that all four potentials predict the specific heat in excellent agreement with experiment [14].

3.3 Surface properties

In Table 4 the results of a number of surface calculations are given. The stacking fault energy is the only quantity here that was initially fit in the development of potential 1. Clearly the predicted value as well as the interplanar expansion is essentially unaffected by potential variation. The calculated free surface energies vary by $\sim 10\%$ between potentials, but in all cases the (111) surface is predicted to have the lowest energy with the (100) and (110) surface energies close in value. The calculated surface energies are in reasonable agreement with the experimental polycrystalline average [15]. By changing the decay length $b^{(h)}$ for the electron density we can bring the free surface relaxation into agreement with experiment. Potentials 1 and 2 predict an increase in near surface interlayer spacing for all of the low index surfaces while potentials 3 and 4 predict a large contraction of the (110) surface, a small contraction for the (100) surface, and a small expansion for the (111) surface in agreement with experiment [16]. We also have calculated the energy of the missing row (110) 2×1 reconstructed surface. Here we find that potentials 1,3, and 4 predict the 1×1 surface to be more stable than the 2×1 in agreement with experiment (see Foiles [17] for a discussion of the (110) reconstruction in fcc metals). Only potential 2 predicts the 2×1 reconstruction in conflict with experiment. It is quite encouraging that potentials 3 and 4 which yield the correct surface relaxation also yield the correct (110) structure.

3.4 Intrinsic defect properties

In Table 5 we present the calculated values for a number of point defects in the fcc structure. The vacancy formation energy is the only quantity fit in the development of potential 1. Potential variation leads to only small (< 0.1 eV) changes in this quantity. For all potentials, the magnitude of the atomic

relaxation around the vacancy is predicted to be below the experimental estimate [18] of -0.3 atomic volumes. The calculated vacancy migration energy is similar for potentials 1-3, but slightly smaller for potential 4. The numbers are in reasonable agreement with experiment [19] indirectly calculated using measured vacancy formation and self diffusion energies. The smaller result for potential 4 is due to a change in the saddle point location. The saddle point for the migration process occurs about halfway between the vacancy and the $\langle 100 \rangle$ split vacancy configurations for potentials 1-3, but at the $\langle 100 \rangle$ split vacancy configuration for potential 4. Thus we see that the range of the potential is important for vacancy migration as previously seen for SiC [8]. We have also calculated the energy of divacancies both at 1st and 2nd neighbor positions. Little effect of potential is seen. The results for first neighbor binding are in reasonable agreement with experiment [20]. Recently Johnson [21] found that vacancy formation energies are significantly altered near a free surface in a 2D model EAM material. He found that the vacancy formation energy was reduced in the first layer, but increased in the second layer. We have investigated this effect for all four potentials for vacancies in the first three layers near low index surfaces. In contrast to Johnson's results for a 2D material we see that the vacancy formation energy in the second layer near (100) and (111) surfaces is the lowest, while near the (110) surface, the 1st layer has the lowest vacancy formation energy. In all cases we see little effect of potential.

There are many possible interstitial configurations. We present the results of the calculations of a few configurations in Table 5. Calculated interstitial formation energies vary a small amount with potential, but in all cases the $\langle 100 \rangle$ split interstitial is predicted to be the minimum energy configuration. The interstitial relaxation volume is in reasonable agreement with experiment [18]. The interstitial migration energy is found to be quite similar for potentials 1-3, but significantly smaller for potential 4. Again as noted above for the vacancy, this difference may be attributed to a shift in saddle point. Potentials 1-3 predict a saddle point about halfway between the O_h and $\langle 100 \rangle$ split configurations, but potential 4 predicts the O_h configuration to be the saddle point. Thus, for both vacancy and interstitial migration we find the range of the potential to be quite important. The calculated interstitial migration energy is significantly above the experimental value [22] for potentials 1-3, but much closer for potential 4.

4.0 Summary

The MEAM is an empirical modification of the EAM which allows angular forces to be included. We have compared the behavior of a model material, Ni, with small angular forces described by four different MEAM potentials by calculating over 50 properties. In general it is found that the vast majority of properties are essentially unaffected by the potential variations. However, there are a number of significant exceptions. It is found that two of the electron density decay parameters strongly control surface relaxations, but do not significantly affect any other properties. The form of the background electron density function is found to affect only the relative stability of the missing row reconstructed (110) surface. The range of the potential is found to be important for the bcc cohesive energy, the thermal expansion coefficient, and the vacancy and interstitial migration energies. These calculations have led us to a new MEAM potential for Ni (potential 4) that reproduces quantitatively all of the experimental data that we have examined.

Acknowledgment

This work was supported by the US Department of Energy.

References

- [1] M.S. Daw, S.M. Foiles, and M.I. Baskes, *Mater. Sci. Rep.*, 9 (1993) 251-310.
- [2] A.E. Carlsson, *Beyond Pair Potentials in Elemental Transition Metals and Semiconductors* Solid State Physics: Advances in Research and Applications, ed. H Ehrenreich and D Turnbull Vol. 43, 1990, Academic Press, Boston.
- [3] M.I. Baskes, *Phys. Rev. Lett.*, 59 (1987) 2666-2669.
- [4] M.I. Baskes, J.S. Nelson, and A.F. Wright, *Phys. Rev. B*, 40 (1989) 6085-100.
- [5] M.I. Baskes, *Phys. Rev. B*, 46 (1992) 2727-2742.

- [6] M.I. Baskes and R.A. Johnson, *Modelling Simul. Mater. Sci. Eng.*, 2 (1994) 147-63.
- [7] M.I. Baskes in *Computational Material Modeling*, A K Noor and A Needleman (eds.) ASME, New York, 1994, p. 23-35.
- [8] H. Huang, N.M. Ghoniem, J.K. Wong, and M.I. Baskes, *Modelling Simul. Mater. Sci. Eng.*, 3 (1995) 615-628.
- [9] M.I. Baskes 1996 *Modified Embedded Atom Method Calculations of Interfaces in International Workshop on Computer Modelling and Simulations for Materials Design* (Tsukuba, Japan) ed S Nishijima and H Onodera 1-9.
- [10] M.I. Baskes, J.E. Angelo, and C.L. Bisson, *Modelling Simul. Mater. Sci. Eng.*, 2 (1994) 505-518.
- [11] M.S. Daw and M.I. Baskes, *Phys. Rev. Lett.*, 50 (1983) 1285-1288.
- [12] J.H. Rose, J.R. Smith, F. Guinea, and J. Ferrante, *Phys. Rev. B*, 29 (1984) 2963-2969.
- [13] R.J. Ravelo and M.I. Baskes in *Thermodynamics And Kinetics Of Phase Transformations*, J S Im, *et al.* (eds.) MRS, Pittsburgh, PA, 1996.
- [14] E.A. Brandes (eds.), *Smithells Metals Reference Book*, 6th ed. Butterworths, London, 1983.
- [15] W.R. Tyson and W.A. Miller, *Surf. Sci.*, 62 (1977) 267-276.
- [16] J.E. Demuth, P.M. Marcus, and D.W. Jepsen, *Phys. Rev. B*, 11 (1975) 1460.
- [17] S.M. Foiles, *Surf. Sci.*, 191 (1987) L779.
- [18] O. Bender and P. Ehrhart in *Point Defects and Defect Interactions in Metals*, J Takamura, M Doyama, and M Kiritani (eds.) North-Holland, Amsterdam, 1982, p. 639.
- [19] H. Bakker, *Phys. Stat. Sol.*, 28 (1968) 569.
- [20] H. Kronmüller in *Vacancies and Interstitials in Metals*, A Seeger, *et al.* (eds.) North-Holland, Amsterdam, 1970, p. 183.
- [21] R.A. Johnson, *Surf. Sci.*, 355 (1996) 241.
- [22] F.W. Young, *J. Nucl. Mater.*, 69&70 (1978) 310.
- [23] N. Saunders, A.P. Miodownik, and A.T. Dinsdale, *CALPHAD*, 12 (1988) 351-374.

- [24] J.P. Hirth and J. Lothe, *Theory of Dislocations* second ed. 1982, John Wiley and Sons, New York.
- [25] A. Seeger, D. Schumacher, W. Schilling, and J. Diehl (eds.), *Vacancies and Interstitials in Metals*, North-Holland, Amsterdam, 1970.
- [26] R.W. Balluffi, *J. Nucl. Mater.*, 69&70 (1978) 240.

TABLES

Table 1: Common parameters for all potentials. The units for E_C are eV and for r_e , r_c , and Δr are Å.

E_C	r_e	a	A	$b^{(0)}$	$b^{(2)}$	$t^{(1)}$	$t^{(2)}$	$t^{(3)}$	C_{\max}	r_c	Δr
4.45	2.49	4.99	1.10	2.45	6.0	3.57	1.60	3.70	2.8	4.0	0.1

Table 2: Parameters for the four potentials.

potential	$b^{(1)}$	$b^{(3)}$	C_{\min}	$G(\Gamma)$
1	2.2	2.2	2.0	Eq. (12a)
2	2.2	2.2	2.0	Eq. (12c)
3	1.5	1.5	2.0	Eq. (12c)
4	1.5	1.5	0.8	Eq. (12c)

Table 3: Comparison of calculated bulk properties. Properties marked with an asterisk were fit in the development of potential 1. Experimental values are presented for reference. All quantities are fully relaxed and calculated at 0 K except for the coefficient of thermal expansion and specific heat which are calculated near room temperature. The coefficient of thermal expansion is the only quantity that significantly depends upon potential.

property	structure	potential				experiment
		1	2	3	4	
cohesive energy (eV)*	fcc	4.45	4.45	4.45	4.45	4.45 ^a
cohesive energy (eV)	hcp	4.43	4.43	4.43	4.43	4.43 ^b
cohesive energy (eV)*	bcc	4.36	4.36	4.36	4.23	4.36 ^b
cohesive energy (eV)	sc	4.07	4.07	4.07	4.06	
cohesive energy (eV)	dc	3.35	3.32	3.34	3.34	
nearest neighbor distance (Å)*	fcc	2.49	2.49	2.49	2.49	2.49 ^a
nearest neighbor distance (Å)	hcp	2.48	2.48	2.48	2.48	
nearest neighbor distance (Å)	bcc	2.39	2.39	2.39	2.45	
nearest neighbor distance (Å)	sc	2.33	2.33	2.33	2.34	
nearest neighbor distance (Å)	dc	2.33	2.34	2.32	2.32	
c/a	hcp	1.65	1.65	1.65	1.65	
bulk modulus (eV/Å ³)*	fcc	1.13	1.13	1.13	1.14	1.15 ^a
shear modulus (eV/Å ³)*	fcc	0.78	0.78	0.78	0.79	0.76 ^a
second shear modulus (eV/Å ³)*	fcc	0.32	0.32	0.32	0.33	0.29 ^a
coefficient of expansion (10⁻⁶ K⁻¹)	fcc	3.66	3.58	2.11	12.38	13.3^a
specific heat (meV K ⁻¹)	fcc	0.26	0.26	0.24	0.27	0.28 ^a

^aReference [14]

^bReference [23]

Table 4: Comparison of calculated surface properties. Properties marked with an asterisk were fit in the development of potential 1. Relaxations are changes in the relative spacing between first and second surface layers or the two layers at the stacking fault. Experimental surface energy is the polycrystalline average. All quantities are taken from fully relaxed configurations at 0 K. The surface relaxations and reconstruction are the only quantities that depend significantly upon potential.

property	potential				experiment
	1	2	3	4	
(111) energy (mJ/m ²)	2014	2182	2217	2216	
(100) energy (mJ/m ²)	2423	2677	2701	2698	2240 ^a
(110) energy (mJ/m ²)	2371	2607	2595	2593	
(111) relaxation (%)	2.72	3.35	0.43	0.43	-1±1^b
(100) relaxation (%)	2.53	3.56	-0.74	-0.74	1±1^b
(110) relaxation (%)	3.81	4.24	-6.94	-6.94	-8±1^b
(110) 2x1 relative energy (mJ/m²)	39	-227	78	51	>0
(111) stacking fault energy (mJ/m ²)*	123	123	124	124	125 ^c
(111) stacking fault relaxation (%)	0.31	0.31	0.27	0.27	

^a Reference [15]

^c Reference [24]

^b Reference [16]

Table 5: Comparison of calculated point defect properties. Properties marked with an asterisk were fit in the development of potential 1. Volume relaxations are changes in volume per atomic volume of nickel. All quantities are taken from fully relaxed configurations at 0 K. The vacancy and interstitial migration energies are the only quantities that depend significantly upon potential.

property	potential				experiment
	1	2	3	4	
vacancy formation energy (eV)*	1.42	1.44	1.48	1.48	1-4-1.6 ^a
vacancy relaxation ($\Delta V/\Omega$)	-0.11	-0.10	-0.12	-0.08	-0.3 ^b
vacancy migration energy (eV)	1.50	1.52	1.49	1.22	1.3-1.5^c
di-vacancy binding energy (1st neighbor) (eV)	0.34	0.23	0.21	0.21	0.33 ^d
di-vacancy binding energy (2nd neighbor) (eV)	0.05	0.07	0.08	0.08	
vacancy 1st layer (100) (eV)	0.49	0.49	0.48	0.48	
vacancy 2nd layer (100) (eV)	0.44	0.32	0.31	0.31	
vacancy 3rd layer (100) (eV)	1.41	1.43	1.48	1.48	
vacancy 1st layer (111) (eV)	0.88	1.01	0.99	1.00	
vacancy 2nd layer (111) (eV)	0.66	0.60	0.59	0.60	
vacancy 3rd layer (111) (eV)	1.40	1.42	1.48	1.48	
vacancy 1st layer (110) (eV)	0.35	0.21	0.28	0.28	
vacancy 2nd layer (110) (eV)	0.65	0.56	0.59	0.49	
vacancy 3rd layer (110) (eV)	0.87	0.84	0.84	0.84	
O _h interstitial formation energy (eV)	4.24	4.27	4.16	4.54	
T _d interstitial formation energy (eV)	5.23	5.26	5.18	5.56	
<100> split interstitial formation energy (eV)	4.04	4.06	3.90	4.24	
<100> split interstitial formation volume ($\Delta V/\Omega$)	1.45	1.44	1.56	2.13	1.7±0.3 ^b
<110> split interstitial formation energy (eV)	5.05	5.08	4.97	5.59	
<111> split interstitial formation energy (eV)	5.55	5.61	5.59	4.66	
interstitial migration energy (eV)	0.68	0.70	0.70	0.28	0.15^e

^a Reference [25, 26]

and the self diffusion energy [19]

^b Reference [18]

^d Reference [20]

^c Using the above vacancy formation energy

^e Reference [22]

FIGURES

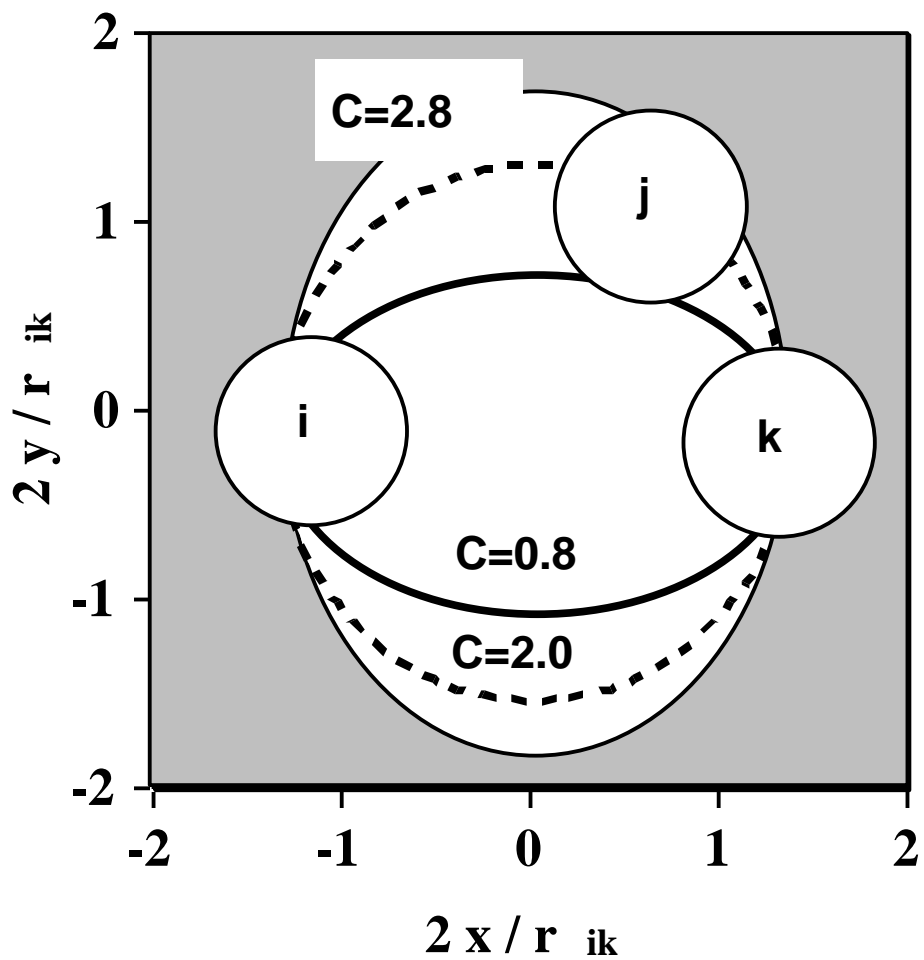


Figure 1: Potential screening of atoms i and k by atom j . Atoms in the shaded region (bounded by $C=2.8$) do not screen atoms i and k , while those inside the full (dashed) curve screen atoms i and k completely for $C_{\min}=0.8$ (2.0). Coordinates are scaled by half of the distance between atoms i and k , r_{ik} .

UNLIMITED RELEASE

INITIAL DISTRIBUTION

U. S. Department of Energy
Office of Basic Energy Sciences
Attn: A. L. Dragoo
Washington, D.C. 20545

U. S. Department of Energy
Office of Basic Energy Sciences
Attn: Iran L. Thomas
Washington, D.C. 20545

U. S. Department of Energy
Office of Basic Energy Sciences
Attn: R. Gottschall
Washington, D.C. 20545

Alcoa Technical Center
Alloy Technology Division
Alcoa Laboratories
Attn: Barbara O. Hall
Alcoa Center, PA 15069

AT&T Bell Laboratories
Attn: M. J. Cardillo
Murray Hill, NJ 07974

AT&T Bell Laboratories
Attn: Y. C. Chabal
Murray Hill, NJ 07974

AT&T Bell Laboratories
Attn: D. R. Hamann
Murray Hill, NJ 07974

AT&T Bell Laboratories
Attn: J. C. Tully
Murray Hill, NJ 07974

Abteilung für Oberflächenchemie
und Katalys
Universität Ulm
Attn: R. J. Behm
Albert-Einstein-Allee 11
D-89081 Ulm/Donau
Federal Republic of Germany

Ames Laboratory
Iowa State University
221 Metals Development
Attn: J. H. Rose
Ames, IA 50011

Arizona State University
Dept. of Materials Science
Attn: J. B. Adams
Tucson, AZ 85721

Argonne National Laboratory
9700 S. Cass Avenue
Attn: D. M. Gruen
Argonne, IL 60439

Argonne National Laboratory
Materials Science Division
Bldg. 212
Attn: Dr. Dieter Wolf
9700 S. Cass Avenue
Argonne, IL 60439

Battelle Pacific Northwest
Attn: R. H. Jones
P. O. Box 999
Richland, WA 99352

Brookhaven National Laboratory
Attn: J. W. Davenport
Upton, Long Island, NY 11973

Brookhaven National Laboratory
Attn: D. Welch
Upton, Long Island, NY 11973

Brown University
Department of Physics
Attn: P. J. Estrup
Providence, RI 02912

Dr. R. Bullough
Materials Development Div.
B552 Harwell Laboratory
Oxfordshire OX11 0RA
England

California Inst. of Technology
Attn: T. C. McGill
Pasadena, CA 91125

California Inst. of Technology
Attn: T. Tombrello
Pasadena, CA 91125

California Inst. of Technology
Attn: W. H. Weinberg
Pasadena, CA 91125

Carnegie-Mellon University
Attn: P. Wynblatt
Dept of Met. Engr. and
Matls. Science
3325 Science Hall
Pittsburgh, PA 15213

Cornell University
Laboratory of Atomic and
Solid State Physics
Attn: N. W. Ashcroft
Ithaca, NY 14853-2508

Cornell University
Bard Hall
Attn: J. M. Blakely
Ithaca, NY 14850

Cornell University
School of Chemical Engineering
Attn: Prof. Paulette Clancy
Olin Hall
Ithaca, NY 14853-1501

Cornell University
Dept. of Materials Science
and Engineering
Attn: Prof. S. L. Sass
Ithaca, NY 14853-1501

Eastman Kodak Company
Research Laboratories, Bldg. 81
Attn: Dr. J. R. Lavine
Rochester, NY 14650-2008

Eindhoven University
Attn: H. H. Brongersma
Dept. of Physics
P. O. Box 513
5600 M. B. Eindhoven
The Netherlands

Fritz-Haber Institut
Faradayweg 4-6
Attn: G. Ertl
1000 Berlin 33
Federal Republic of Germany

Fysik Institut
Odense Universitat
Attn: P. Sigmund
DK-5230 Odense M
Denmark

George Washington University
School of Engineering and Applied Science
Attn: Charles Gilmore
Associate Dean for Research
Tompkins Hall
Washington, D. C. 20052

Georgia Institute of Technology
Attn: Prof. Uzi Landman
225 North Avenue N.W.
Atlanta, GA 30332

Hahn-Meitner-Institut
Attn: H. Wollenberger
Glienicke Str. 100
1000 Berlin 39, West Germany

Harvard University
Attn: Prof. H. Ehrenreich
Cambridge, MA 02183

Harvard University
Attn: Prof. J. R. Rice
Cambridge, MA 02183

Haverford College
Department of Physics
Attn: L. Roelofs
Haverford, PA 19041

IBM
Almaden Research
K33.801
Attn: Farid F. Abraham
650 Harry Road
San Jose, CA 95120-6099

IBM
Fishkill Laboratory
Dept. 62G
Attn: Dr. Cheruvu S. Murthy
Hopewell Junction, NY 12533

IBM.
T. J. Watson Research Center
Attn: P. M. Marcus
P. O. Box 218
Yorktown Heights, NY 10598

IBM.
T. J. Watson Research Center
Attn: J. Tersoff
P. O. Box 218
Yorktown Heights, NY 10598

Institut für Festkörperforschung
der Kernforschungsanlage
Attn: P. H. Dederichs
Postfach 1913
D-5170 Jülich 1, West Germany

Institut für Festkörperforschung
der Kernforschungsanlage
Attn: H. Ibach
Postfach 1913
D-5170 Jülich 1, West Germany

Institut für Festkörperforschung
der Kernforschungsanlage
Attn: W. Schilling
Postfach 1913
D-5170 Jülich 1, West Germany

Institut für Festkörperforschung
der Kernforschungsanlage
Attn: H. Wenzl
Postfach 1913
D-52405 Jülich, Germany

Institut für Physikalische Chemie
Freie Universität Berlin
Attn: K. Christman
Takush. 3
1000 Berlin 33
Federal Republic of Germany

Institute of Corrosion and Protection of
Metals Academia Sinica
No. 62 Wencui Road
Shenyang 110015
China

Interfaculty Reactor Institute
Attn: Dr. A. van Veen
Mekelweg 15
NL-2629JB, Delft
The Netherlands
International School for
Advanced Studies
Attn: Prof. F. Ercolessi
I-34014 Trieste
Italy

International School for
Advanced Studies
Attn: E. Tosatti
I-34014 Trieste
Italy

Iowa State University
Ames Laboratory
Attn: A. E. DePristo
Ames, IA 50011

Iowa State University
Ames Laboratory
Attn: K.-M. Ho
Ames, IA 50011

Iowa State University
Ames Laboratory
Attn: P. A. Thiel
Ames, IA 50011

Professor Ryoichi Kikuchi
1702 Comstock Dr.
Walnut Creek, CA 94595-2469

Lab. Voor Fysische Metaalkunde
Materials Science Centre
Attn: J. Th. M. De Hosson
Groningen, Nijenborgh 18
The Netherlands

Lawrence Berkeley Laboratory
Materials and Molecular Res. Div.
Attn: M. L. Cohen
Berkeley, CA 94720

Lawrence Berkeley Laboratory
Materials and Molecular Res. Div.
Attn: S. G. Louie
Berkeley, CA 94720

Lawrence Berkeley Laboratory
Materials and Molecular Res.Div.
Attn: G. A. Somorjai
Berkeley, CA 94720

Lawrence Berkeley Laboratory
Attn: A. W. Thompson
One Cyclotron Road, MS 66-203
University of California
Berkeley, CA 94720

Lawrence Berkeley Laboratory
Materials and Molecular Res. Div.
Attn: M. A. van Hove
Berkeley, CA 94720

Lockheed Martin Idaho Technologies
Attn: Clint Van Siclen
P. O. Box 1625
Idaho Falls, ID 83415-2211

Los Alamos Natl. Scientific Lab.
P. O. Box 1663
Attn: S. P. Chen
Los Alamos, NM 87545

Los Alamos Natl. Scientific Lab.
Attn: Dr. Terry C. Lowe
MST-5, MS G730
P.O. Box 1663
Los Alamos, NM 87545

Los Alamos Natl. Scientific Lab.
P. O. Box 1663
Attn: A. Voter
Los Alamos, NM 87545

Loyola College
Department of Physics
Attn: Prof. R. S. Jones
4501 N. Charles St.
Baltimore, MD 21210

Massachusetts Inst. of Technology
Attn: Prof. A. S. Argon
Cambridge, MA 02139

Massachusetts Inst. of Technology
Attn: Prof. R. M. Latanision
Cambridge, MA 02139

Massachusetts Inst. of Technology
Attn: S. Yip
Cambridge, MA 02139

Max-Planck-Institut für Plasmaphysik
Attn: R. Behrisch
D8046 Garching, West Germany

Max-Planck-Institut für Plasmaphysik
Attn: Professor V. Dose
D-8046 Garching, West Germany

Max-Planck-Institut für Metallforschung
Institut für Werkstoffwissenschaften
Attn: Prof. Dr. Phil. H. Fischmeister
Seestrasse 92
7000 Stuttgart 1
Federal Republic of Germany

Max-Planck-Institut für Metallforschung
Institut für Werkstoffwissenschaft
Attn: Dr. S. Schmauder
Seestrasse 92
70174 Stuttgart
Federal Republic of Germany

Max-Planck-Institut für
Stromungsforschung
Attn: Prof. J. P. Toennies
Bunsenstrasse 10
D-3400 Göttingen
Federal Republic of Germany

Michigan Technological University
Dept. of Metallurgical Engineering
Attn: J. K. Lee
Houghton, MI 49931

Mitsubishi Heavy Industries, Ltd.
Attn: Ohira Tatsuya
Advanced Technology Research Center
Technical Headquarters
8-1, Sachiura 1-chome
Kanazawa-ku, Yokohama
236 Japan

National Institute of Standards
and Technology
Attn: J. M. Rowe, 235/A106
Washington, DC 20234

National Institute of Standards
and Technology
Materials Bldg., Rm. A 113
Attn: R. Thomson
Washington, DC 20234

National Research Institute
for Metals
Computational Matls. Science Div.
Attn: Katsuyuki Kusunoki, Dr. Eng.
1-2-1 Sengen, Tsukuba
305. JAPAN

Naval Research Laboratory
Attn: T. Andreadis, Code 4651
Washington, DC 20375

Naval Research Laboratory
Attn: Michael J. Mehl, Code 4693
4555 Overlook Ave. SW
Washington, DC 20375-5000

Nippon Steel Corporation
Attn: Dr. Tooru Matsumiya
Advanced Materials & Technology Research
Laboratories
1618 Ida. Nakahara-ku
Kawasaki 211, Japan

North Carolina State University
Attn: Dr. J. Narayan
Department of Materials and Eng.
Raleigh, NC 27607

Northwestern University
Dept. of Mat. Science & Eng.
Attn: Dr. David Seidman
2145 Sheridan Road
Evanston, IL 60201-9990

Oak Ridge National Laboratory
Bldg. 4500S, MS 6114
Box 2008
Attn: W. H. Butler
Oak Ridge, TN 37831-6114

Oak Ridge National Laboratory
P. O. Box X
Attn: H. L. Davis
Oak Ridge, TN 37830

Oak Ridge National Laboratory
P.O. Box 2008
Attn: D. Pedraza
Oak Ridge, TN 37831-6069

Oak Ridge National Laboratory
P. O. Box X
Attn: J. O. Steigler
Oak Ridge, TN 37830

Oak Ridge National Laboratory
P. O. Box X
Attn: M. Stocks
Oak Ridge, TN 37830

Oak Ridge National Laboratory
Attn: M. H. Yoo
Metals and Ceramics Division
P. O. Box 2008, Bldg. 5500, MS-6376
Oak Ridge, TN 37830

The Ohio State University
Division of Materials Research
Attn: S. A. Dregia
Columbus, OH 43210-1106

The Ohio State University
Attn: Prof. P. Shewmon
Dept. Matl. Sci. & Engr.
116 W. 19th Ave.
Columbus, OH 43210-1106

The Ohio State University
Physics Department
Attn: J. W. Wilkins
174 West 18th Avenue
Columbus, OH 43210-1106

Oxford University
Attn: Prof. D. G. Pettifor
Parks Road
Oxford OX1 3PH
England

Oxford University
Dept. of Metallurgy and
Science of Materials
Attn: Adrian Sutton
Parks Road
Oxford OX1 3PH
England

Pennsylvania State University
Attn: Barbara J. Garrison
Department of Chemistry
State College, PA 16801

Queens University
Dept. of Physics
Attn: Prof. Malcolm Stott
Stirling Hall
Kingston, Canada K7L 3N6

Rice University
Attn: Prof. R. B. McLellan
Houston, TX 77251

Rutgers University
Dept. of Ceramics
Attn: Dr. S. H. Garofalini
P. O. Box 909
Piscataway, NJ 08854

School of Mathematics and Physics
Queen's University of Belfast
Attn: M. W. Finnis
Belfast BT7 1NN
Northern Ireland

Seagate Technology
Attn: Prof. James Angelo
8001 East Bllomington Fwy.
Bloomington, MN 55420

Stanford University
Department of Chemistry
Attn: Hans C. Anderson
Stanford, CA 94305

Stanford University
Department of Materials Science & Engineering
Attn: Timur Halicioglu
Stanford, CA 94305

Stanford University
Dept. of Chemical Engineering
Attn: Prof. R. Madix
Stanford, CA 94305

Stanford University
Department of Chemistry
Attn: Prof. R. Zare
Stanford, CA 94305

Technical University of Denmark
Attn: J. K. Nørskov
Lab. f. Technical Physics
DK-2800 Lyngby, Denmark

Texas A&M University
Dept. of Nuclear Engineering
Attn: Dr. R. Vijay
College Station, TX 77843

Ukrainian Academy of Sciences
Attn: V. Pokropivny
V. Ogorodnikov
Institute for Problems of Matls. Science
Computer Simulation Laboratory
Ukrainian 252680 KIEV GSP-142

University of Aarhus
Institute of Physics
Attn: F. Besenbacher
DK-8000 Aarhus C, Denmark

University of Aarhus
Institute of Physics
Attn: J. Bottiger
Ivan Stensgaard
DK-8000 Aarhus C, Denmark

University of California
MANE Department
Attn: N. M. Ghoniem
6275 Boelter Hall
Los Angeles, CA 90024

University of California, Berkeley
Department of Materials Science & Mineral
Engineering
Attn: Prof. D. C. Chrzan
577 Evans
Berkeley, CA 94720

University of California, Irvine
Department of Physics
Attn: Prof. A. Maradudin
Irvine, CA 92717

University of California, Irvine
Department of Physics
Attn: Prof. M. Mills
Irvine, CA 92717

University of Connecticut
Center for Materials Simulation
Attn: Professor Phil Clapp
97 North Eagleville Rd.
Storrs, CT 06269-3136

University of Connecticut
Department of Metallurgy
Attn: Jonathan A. Rifkin
97 North Eagleville Rd.
U-136
Storrs, CT 06269-3136

University of Copenhagen
H. C. Ørsted Institute
Attn: H. H. Andersen
Universitetsperken 5
DK-2100 Copenhagen, Denmark

University of Illinois
Dept. of Materials Science
Attn: J. B. Adams
Urbana, IL 61801

University of Illinois
Dept. of Mining and Metallurgy
Attn: H. K. Birnbaum
Urbana, IL 61801

University of Illinois
Nuclear Eng. Lab.
Attn: D. Ruzic
103 S. Goodwin Ave., Rm. 214
Urbana, IL 61801

The University of Liverpool
Dept. of Materials Science
and Engineering
Attn: Prof. D. J. Bacon
P. O. Box 147
Liverpool L69 3BX
England

University of Maryland
Department of Physics
Attn: T. Einstein
College Park, MD 20742-4111

University of Maryland
Department of Physics
and Astronomy
Attn: Dr. K. E. Khor
College Park, MD 20742-4111

University of Michigan
Dept. of Mat. Sci. and Engr.
Attn: D. Srolovitz
Ann Arbor, MI 48109-2136

University of Michigan
Dept. of Nuclear Engineering
Attn: G. Was
Ann Arbor, MI 48109

University of Minnesota
Dept. of Chemical Engr. and
Materials Science
Attn: J. R. Chelikowsky
151 Amundson Hall
421 Washington Avenue S. E.
Minneapolis, MN 55455

University of Minnesota
Corrosion Research Center
Attn: W. W. Gerberich
Minneapolis, MN 55455

University of Minnesota
Corrosion Research Center
Attn: R. A. Oriani
Minneapolis, MN 55455

University of New Mexico
Chemistry & Nuclear Eng. Dept.
Attn: Dr. Anil Prinja
Albuquerque, NM 87131

University of Notre Dame
Dept. Physics
Attn: J. Dow
Box E
Notre Dame, IN 46556

University of Pennsylvania
Department of Materials Science
Attn: V. Vitek
Philadelphia, PA 19104

University of Texas
Depts. of Astronomy & Physics
RLM 15-212
Attn: R. Smoluchowski
Austin, TX 78712

University of Trieste
Dipartimento di Fisica Teorica
Attn: Prof. N. Parrinello
I-34014 Trieste
Italy

University of Virginia
Department of Materials Science
Attn: R. A. Johnson
School of Engineering and
Applied Science
Charlottesville, VA 22901

University of Wisconsin
ECE Department
Attn: Prof. W. N. G. Hitchon
Madison, WI 53706

Vanderbilt University
Dept. of Mechanical Engineering
Attn: Prof. William F. Flangan
Box 1592, Station B
Nashville, TN 37235

Virginia Commonwealth University
Dept. of Physics
Attn: Prof. P. Jena
Richmond, VA 23284-2000

Virginia Commonwealth University
Dept. of Physics
Attn: Prof. T. McMullen
Richmond, VA 23284-2000

Virginia Polytechnic Institute and University
Department of Materials Science and Eng.
Attn: Yri Mishin
Blacksburg, VA 24061

Virginia Tech
Materials Engineering Dept.
Attn: Prof. Diana Farkas
213 Holden
Blacksburg, VA 24061-0237

Washington University
Department of Physics
Campus Box 1105
Attn: Anders Carlsson
St. Louis, MO 63130

Washington State University
Dept. of Mechanical and
Materials Engineering
Attn: Richard Hoagland
Pullman, WA 99164-2920

Westinghouse Savannah River Co.
Attn: Ralph Wolf
Scientific Computation Section
Bldg. 773-42A
Aiken, SC 29802

Westinghouse Electric Corporation
Bettis Atomic Power Laboratory
Attn: Richard W. Smith
Post Office Box 79
West Mifflin, PA 15122-0079

West Virginia University
Dept. of Physics
Attn: Bernard R. Cooper
Morgantown, WV 26506

A. Gonis, L-268
W. E. King, L-356
M. J. Weber, L-326

MS 0149 D. L. Hartley, 4000
MS 0161 B. W. Dodson, 11500
MS 0457 H. W. Schmitt, 2000
MS 0513 R. J. Eagan, 1000
MS 0601 J. S. Nelson, 1113
MS 1056 S. M. Myers, 1112
MS 1056 B. L. Doyle, 1111
MS 1056 W. R. Wampler, 1111
MS 1079 A. D. Romig, 1300
MS 1320 W. G. Perkins, 6832
MS 1349 T. P. Swiler, 1846
MS 1405 E. A. Holm, 1841
MS 1411 F. Yost, 1841
MS 1413 D. R. Jennison, 1114
MS 1413 G. L. Kellogg, 1114

MS 1413 T. A. Michalske, 1114
 MS 1423 G. C. Osbourn, 1155
 MS 1427 S. T. Picraux, 1100

MS 9001 T. O Hunter, 8000
 Attn: J. B. Wright, 2200
 M. E. John, 8100
 L. A. West 8200
 W. J. McLean, 8300
 R. C. Wayne, 8400
 P. N. Smith, 8500
 P. E. Brewer, 8800
 D. L. Crawford, 8900

MS 9052 M. Allendorf, 8361
 MS 9108 S. L. Robinson, 8412
 MS 9161 K. L. Wilson, 8716
 MS 9161 M. D. Asta, 8717
 MS 9161 S. M. Foiles, 8717
 MS 9161 A. A. Quong, 8717
 MS 9161 W. G. Wolfer, 8717
 MS 9163 W. Bauer, 8302
 MS 9214 C. F. Melius, 8117
 MS 9401 M. T. Dyer, 8700
 Attn: J. C. F. Wang, 8713
 G. J. Thomas, 8715
 E. P. Chen, 8742
 P. E. Nielan, 8743
 W. A. Kawahara, 8746

MS 9402 M. W. Perra, 8711
 MS 9403 M. I. Baskes, 8712 (50)
 MS 9403 S. E. Guthrie, 8712
 MS 9403 N. R. Moody, 8712
 MS 9409 G. D. Kubiak, 8250
 MS 9409 R. H. Stulen, 8250
 MS 9904 W. D. Wilson, 8700

MS 0899 Technical Library, 4414 (4)
 MS 9021 Technical Communications Dept.
 8815/Technical Library,
 MS0899, 4414

MS 9018 Central Technical Files,
 8940-2 (3)